Am J Transl Res 2023;15(7):4687-4698
www.ajtr.org /ISSN:1943-8141/AJTR0149236

Original Article

Clinicopathological significance of vasculogenic mimicry and fetal hemoglobin expression in peripheral neuroblastic tumors in children

Aihua Zhang[1], Shiwu Zhang[2]

[1]*Graduate School, Tianjin Medical University, Tianjin, China;* [2]*Department of Pathology, Tianjin Union Medical Center, Tianjin, China*

Received January 18, 2023; Accepted June 29, 2023; Epub July 15, 2023; Published July 30, 2023

Abstract: Purpose: Vasculogenic mimicry (VM) is present in a variety of malignant tumors, and is related to the degree of malignancy. Neuroblastoma (NB) can induce the expression of fetal hemoglobin (HB-F). The purpose of this study was to investigate the clinicopathological significance of the number of VMs and tumor cell expression of HB-F in children with peripheral neuroblastic tumors (pNTs). Materials and Methods: We collected tissue samples and clinical data from 101 children with pNTs; prepared serial sections of tissue wax blocks for hematoxylin and eosin staining, CD31/periodic acid-Schiff double staining, and HB-F immunohistochemical staining; and analyzed the experimental results. Results: There were significant differences in the number of VMs and HB-F expression in tumor cells according to the pathological classification of pNTs (P<0.001, collectively). Poorly differentiated NB had a median of 137 VMs and 25.5% HB-F expression. Differentiating NB had a median of 90.5 VMs and 8.5% HB-F expression. Ganglioneuroblastoma intermixed had a median of 6.0 VMs and 1.0% HB-F expression. Ganglioneuromas had no VM and a median of 0% HB-F expression. The number of VMs and the expression of HB-F were significantly higher in the poor prognosis group than the good prognosis group (P<0.001, collectively). There was a strong positive correlation between the number of VMs and HB-F expression in pNTs (r=0.891, P<0.001). Conclusion: We confirmed VM and HB-F expression in pNTs. The number of VMs and HB-F expression were higher in poorly differentiated tumors. The number of VMs and level of HB-F expression in pNTs might be related to the prognosis.

Keywords: Peripheral neuroblastic tumors, vasculogenic mimicry, fetal hemoglobins

Introduction

Peripheral neuroblastic tumors (pNTs) are a class of extracranial malignant embryonic tumors originating from the primitive neural crest and are one of the most common malignant tumors in children [1, 2]. PNTs account for 15% of malignant tumors deaths in children in North America [3, 4]. The International Neuroblastoma Pathology Committee (INPC) divides pNTs into the following four subtypes: neuroblastoma (NB), ganglioneuroblastoma intermixed (GNBi), ganglioneuroblastoma nodular (GNBn), and ganglioneuroma (GN) [5]. NB can be further divided into three subtypes: undifferentiated (composed of undifferentiated neuroblasts without discernible neuropils); poorly differentiated (the most common subtype, most of which are typical neuroblasts with clearly recognizable neuropils); and differentiating (containing abundant neuropils with differentiation of more than 5% of the neuroblasts) [5, 6]. GNBi tumors contain more than 50% Schwannian stroma, containing neuroblasts at different stages of differentiation. GN are composed mainly of Schwannian stroma scattered with mature or maturing ganglion cells and can be divided into mature and maturing subtypes [5]. The principal feature of GNBn is the presence of one or more obvious neuroblastic nodules (stroma-poor component) coexisting with GN or GNBi. The prognosis of GNBn depends on the tissue classification of the nodules [7]. The prognosis of pNTs is related to a variety of factors, including age, histological type, mitosis-karyorrhexis index (MKI), and molecular genetic changes [8]. The known genetic alterations associated with pNTs include MYCN amplification, 1p deletion

and 11q deletion [9, 10]. In 2003, the INPC modified the prognostic classification, which was divided into two groups: favorable histology (FH) and unfavorable histology (UH) [7, 11, 12]. Cases with UH often progress rapidly, and metastasis may occur in the early stage, causing difficulties in the treatment of children. Approximately 40% of children with high-risk NB eventually die due to treatment failure and recurrence [13, 14]. Therefore, identifying the causes of treatment failure and developing effective new methods of treatment have become the focus of current research.

In recent years, many studies have found that vasculogenic mimicry (VM) is present in many other malignant tumors such as melanoma, ovarian cancer, glioma, breast cancer, liver cancer, and gastric adenocarcinoma [15-20]. VM is a simulated vascular channel formed by tumor cells surrounding erythrocytes [21]. Because the inner wall of the lumen is not covered by endothelial cells, tumor cells can enter the blood directly; therefore, tumors with VM are prone to metastasis and have a poor prognosis [22]. For such tumors, anti-angiogenesis-targeted drugs, such as bevacizumab and sunitinib, are generally ineffective [23-25].

Tumor growth cannot be separated from the oxygen supply. When the tumor grows too rapidly, the lack of oxygen supply to the tumor cells leads to ischemic necrosis. The oxygen-carrying capacity of fetal hemoglobin (HB-F) is higher than that of adult hemoglobin, while its oxygen release capacity is weak [26]. HB-F ensures that tumor cells can survive under severe hypoxia. Previous studies have demonstrated the expression of HB-F in NB using immunohistochemistry [27]; however, its specific expression is not clear. The vascularized tissue-engineered model of NB has also confirmed the existence of VM in vitro [28]; however, it has rarely been reported in natural tumors. In this experiment, 101 pathological specimens of patients with pNTs were collected to verify the existence of VM and HB-F expression in tumors, and to study the relationship and significance between pNTs and VM and HB-F expression.

Materials and methods

Collection and arrangement of pathological materials

Tissue samples were collected from 101 children with pNTs with complete clinical data from April 2006 to January 2022 at Tianjin Children's Hospital. Among the 101 cases, there were 59 NB (1 undifferentiated, 42 poorly differentiated, and 16 differentiating type), 24 GNBi, 2 GNBn, and 16 GN. The age at the time of diagnosis, sex, MKI, prognosis of each case was recorded.

Selection of wax blocks

All original hematoxylin and eosin (H&E)-stained sections from each patient were reviewed. Because of the uneven distribution of cell components in pNTs, we determined typical sections that conformed to the histological classification and determined the corresponding wax blocks. Each wax block was continuously sliced for at least three pieces (3 μm/piece). Three section each was stained using H&E staining, CD31/periodic acid-Schiff (PAS) double staining, and HB-F immunohistochemical staining.

Hematoxylin and eosin staining

The 3-μm sections were deparaffinized and rehydrated, then stained with hematoxylin (Baso, Zhuhai, China) for 5 minutes, differentiated and reblued, stained with eosin (Baso, Zhuhai, China) for 40 seconds, dehydrated with gradient alcohol, and sealed with sealing glue.

CD31/PAS double staining

For CD31/PAS double staining, immunohistochemical staining of the sections was performed using the avidin-biotin-peroxidase method in the earlier stages and incubation with CD31 primary antibody (Long Island, Shanghai, China). After diaminobenzidine (DAB; Long Island, Shanghai, China) developed color, sections were washed with running water, and solution A of the PAS kit (Maiwei, Xiamen, China) was then added for 10 min. The sections were then washed with distilled water, and solution B was added for 15 min, and then they were rinsed with tap water for 10 min. The nucleus was counterstained with hematoxylin and dehydrated, and sealed.

Fetal hemoglobin immunohistochemical staining

The 3-μm sections were deparaffinized and rehydrated, then soaked in 3% H_2O_2 solution for 10 min, washed with water, microwave repaired with pH 6.0 sodium citrate repair solution for

15 min, serum blocked for 30 min, incubated with rabbit anti-hemoglobin subtype γ 2 monoclonal antibody (Bioss, Beijing, China, with dilution ratio of 1:50) overnight at 4°C in a humidified chamber. The next day, the secondary antibody (Celplor, North Carolina, USA) was added to the slices for 30 min, the prepared DAB solution (Long Island, Shanghai, China) was added for color development for 10 min, and the nuclei were counterstained with hematoxylin, dehydrated, and sealed.

HB-F/PAS double staining

HB-F/PAS double staining was performed on sections containing VMs, similar to CD31/PAS double staining, and rabbit anti-hemoglobin subtype γ 2 monoclonal antibody (Bioss, Beijing, China, at a dilution ratio of 1:50) was used as the primary antibody.

HB-F/CD31 double staining

A Leica immunohistochemical instrument was used for HB-F/CD31 double staining of VM and blood vessel sections. HB-F was stained brown using the horseradish peroxidase-DAB method, and CD31 was stained red using the alkaline phosphatase-red method.

Histopathological assessment

The lumen wall cells of the VM were negative for CD31 and positive for PAS or negative for both CD31 and PAS, with red blood cells in the lumen. CD31 and PAS staining were positive in endothelial-dependent vessels. Ten randomly selected hotspot fields of the CD31/PAS double-stained sections were viewed at ×400 magnification, and the total number of VMs in each section was counted. Positive HB-F immunohistochemical staining was seen as brownish yellow fine particles in red blood cells. The HB-F positivity rate was determined by viewing 10 randomly selected hotspot fields ×400 magnification, counting 100 cells in each visual field, calculating the proportion of positive cells in each visual field, and then calculating the mean value for the 10 visual fields.

Classification of peripheral neuroblastic tumors

According to the INPC classification, there is a gradual differentiation and maturation process of tumors from undifferentiated, poorly differentiated, and differentiating NB, to GNBi and GN. As the degree of differentiation and maturation increases, the Schwann stromal component changes from poor to abundant, the primitive neuroblast component gradually decreases, and the increased neuroblasts started to differentiate and mature into ganglion cells. GNBn is a special type and its degree of differentiation shows diversity because of the differences in the composition within the nodule. Therefore, we classified the 101 pNT tissue samples into the following six groups: undifferentiated NB, poorly differentiated NB, differentiating NB, GNBi, GN, and GNBn.

Statistical analysis

SPSS, version 25.0 (IBM Corporation, Armonk, NY, USA) software was used to analyze the data. Because some data in the grouping did not meet the normal distribution, the Mann-Whitney U test was used to test the association of sex and prognosis with VM and HB-F; the Kruskal-Wallis H test was used to test the association of age, differentiation type, and MKI with VM and HB-F; and correlation analysis and partial correlation analysis were used to test the significant of correlations between age, VM, and HB-F. Statistical significance was set at $P<0.05$.

Results

Basic characteristics of the peripheral neuroblastic tumors

We observed the typical histopathological characteristics of each of the six groups of pNTs on microscopy, as shown in **Figure 1A**. Undifferentiated NB were composed of undifferentiated neuroblasts without discernible neuropils (**Figure 1Aa**). Poorly differentiated NB were composed of undifferentiated neuroblastic cells with clearly recognizable neuropils, and some neuroblasts formed a Homer-Wright rosette around the neuropils (**Figure 1Ab**). Differentiating NB showed synchronous nuclear and cytoplasmic differentiation in more than 5% of the neuroblasts (**Figure 1Ac**). GNBi showed well-defined microscopic nests of neuroblastic cells that were intermixed or randomly distributed in >50% of the Schwannian stroma (**Figure 1Ad**). GN showed fully mature ganglion

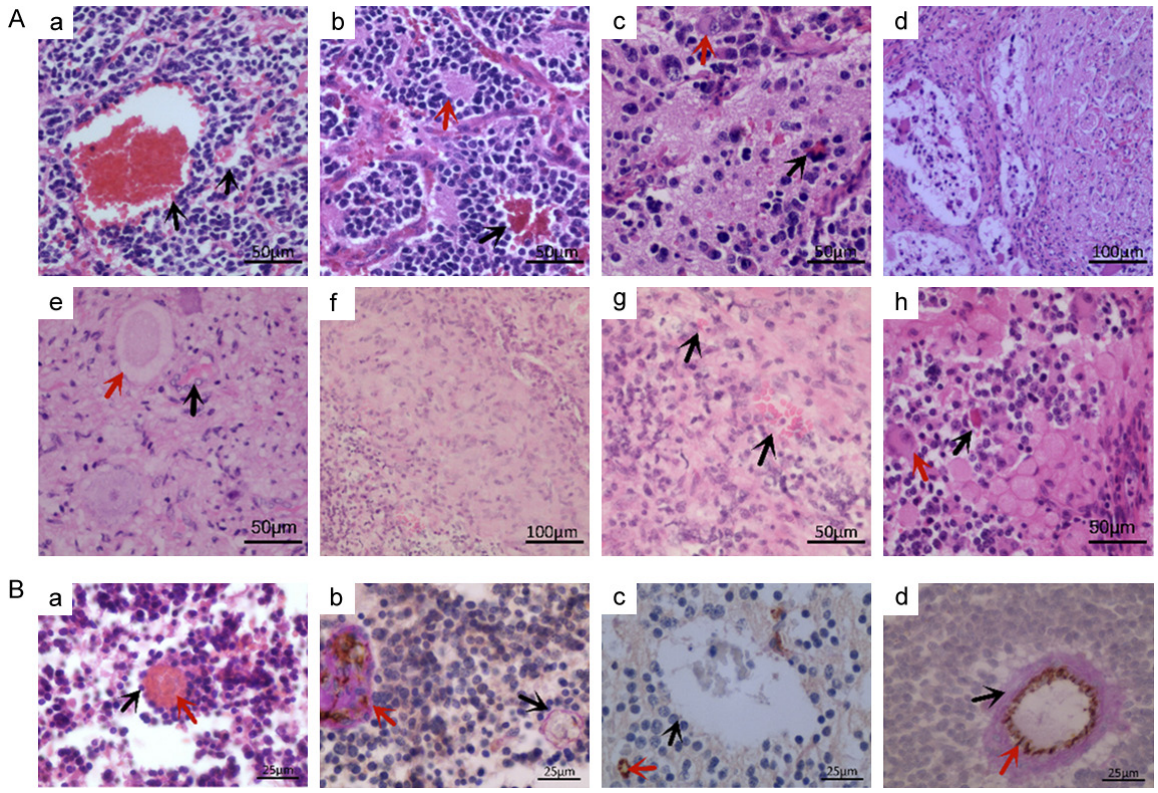

Figure 1. A. Morphological characteristics of different differentiation types of peripheral neuroblastic tumors (pNTs): (a) Undifferentiated neuroblastoma (NB) showing undifferentiated neuroblasts forming vasculogenic mimicry (VM) structures around red blood cells (black arrowheads) (H&E, ×20). (b) Poorly differentiated NB showing a rosette of undifferentiated neuroblasts surrounding the neuropil (red arrowheads) and VM structure (black arrowheads) (H&E, ×20). (c) Differentiating NB showing differentiating neuroblasts (red arrowheads) and the VM structure (black arrowheads) (H&E, ×20). (d) Ganglioneuroblastoma intermixed (GNBi) showing more than 50% Schwann matrix, containing scattered neuroblastoma nests (H&E, ×10). (e) Ganglioneuroma (GN) showing mature ganglion cells (red arrowheads), blood vessel structure (black arrowheads) (H&E, ×20). (f) Ganglioneuroblastoma nodular (GNBn) showing a clear boundary between the neuroblastoma nodules (lower left) and the stroma-rich tumor tissue (upper right) (H&E, ×10). (g) GNBn showing the VM structure in the neuroblastoma nodule (black arrowheads) (H&E, ×20). (h) GNBi showing immature ganglion cells (red arrowheads), and the VM structure (black arrowheads) (H&E, ×20). B. Characteristics of the VM structure: (a) VM structure formed by neuroblasts (black arrowheads) surrounding erythrocytes (red arrowheads) (H&E, ×40). (b) VM structure at the same position under CD31/periodic acid-Schiff (PAS) double staining, showed neuroblast CD31-negative and PAS-positive (black arrowheads), blood vessel nearby (red arrowheads) (CD31/PAS, ×40). (c) VM structure with both CD31-negative and PAS-negative (black arrowheads), blood vessel (red arrowheads) (CD31/PAS, ×40). (d) Endothelium dependent vascular structure with endothelial cells CD31-positive (red arrowheads), PAS-positive (black arrowheads) (CD31/PAS, ×40).

cells with satellite cells that were individually embedded in the Schwannian stroma (**Figure 1Ae**). GNBn showed ganglioneuromatous tissue as thin septa between the NB nodules and the stroma-rich tumor tissue (**Figure 1Af**). The pathological data of children with pNTs in each group are summarized in **Table 1**. We took FH and UH to represent good and poor prognosis. The age distribution was significantly different among the six groups of pNTs (P<0.001, Kruskal-Wallis H test). Differentiation of pNTs increased significantly with increasing age from poorly differentiated NB, differentiating NB, GNBi to GN (**Table 1**). Overall, the number of pNTs did not differ by sex (50 boys, 51 girls); however, girls had better differentiation types (P=0.028, Fisher's exact test). The prognosis of pNTs was associated with the degree of tumor differentiation (P<0.001, Fisher's exact test). MKI was not associated with the degree of tumor differentiation (P=0.361, Fisher's exact test).

Features of vasculogenic mimicry in peripheral neuroblastic tumors

Different numbers of VMs were observed in NB and GNBn (**Figure 1Aa-Ac**, **1Ag**). Of the 24

Table 1. Classification and histopathology of peripheral neuroblastic tumors in study subjects (N=101)

	Undifferentiated NB	Poorly differentiated NB	Differentiating NB	GNBi	GN	GNBn	P
n	1	42	16	24	16	2	
Age/month							
$\bar{x}\pm s$	72	16.3±18.5	24.8±16.5	57.8±37.2	72±24.8	24±17.0	0.000
Gender							
Male	1	28	5	10	6	0	0.028
Female	0	14	11	14	10	2	
Prognosis							
Good	0	28	14	24	16	1	0.000
Poor	1	14	2	0	0	1	
MKI							
Low	1	27	13			1	0.361
Medium	0	11	3			0	
High	0	4	0			1	

Remarks: NB, neuroblastoma; GNBi, ganglioneuroblastoma intermixed; GN, ganglioneuroma; GNBn, ganglioneuroblastoma nodular; MKI, mitosis-Karyorrhexis index.

cases of GNBi, 18 cases had VMs in the GNBi but no VM in the GN (**Figure 1Ae**, **1Ah**). On microscopy, VMs appeared as lumen-like structures composed of small round blue neuroblasts could be seen on H&E staining, and the lumen was full of red blood cells (**Figure 1Ba**). In the same position as the CD31/PAS double staining section, the lumen wall cells were negative for CD31 staining, with or without a layer of continuous pink PAS staining, such as the basement membrane lining the wall (**Figure 1Bb**, **1Bc**). Endothelial cell-dependent vessels were positive for both CD31 and PAS staining and their cell walls were spindle-shaped (**Figure 1Bd**). The VM were distributed predominantly under the tumor capsule and in necrotic areas of the tumor cells.

Expression characteristics of fetal hemoglobin in peripheral neuroblastic tumors

Both NB and GNBn showed high or moderate expression of HB-F in the tumor cells (**Figure 2Aa-Ad**). In the GNBi group, there were 15 cases of low HB-F expression and 9 cases of no expression (**Figure 2Ae**). In the GN group, there were 4 cases of low HB-F expression and 12 cases of no expression (**Figure 2Af**). The expression of HB-F by tumor cells was mostly distributed in front of the tumor invasion (**Figure 2Ba**), around necrotic areas (**Figure 2Bb**), and in VMs (**Figure 2Bc**), but it some blood vessels were negative for HB-F (**Figure 2Bd**).

Relationship between the number of vasculogenic mimicries and clinicopathological indexes in peripheral neuroblastic tumors

There was no significant difference in number of VMs according to sex (P=0.094, **Table 2**); however, there were significant differences in the number of VMs according to the histopathological classification (P<0.001, **Table 2**). Poorly differentiated histopathological types tended to have a greater number of VMs; however, this was not analyzed statistically owing to the small number of cases of undifferentiated NB and GNBn. The number of VMs in poorly differentiated NB was significantly higher than that in other groups; and the number of VMs in differentiating NB was higher than that in GN; whereas there were no differences between differentiating NB and GNBi, or between GNBi and GN (**Table 3**). The number of VMs was significantly higher in the poor prognosis group than in the good prognosis group (P<0.001, **Table 2**). There was no significant difference in the number of VMs according to the MKI (P=0.175, **Table 2**).

Relationship between fetal hemoglobin expression in tumor cells and clinicopathological indexes in peripheral neuroblastic tumors

HB-F expression did not differ significantly according to sex (P=0.062, **Table 4**), but differed significantly according to the histopathological classification (P<0.001, **Table 4**). Poorly

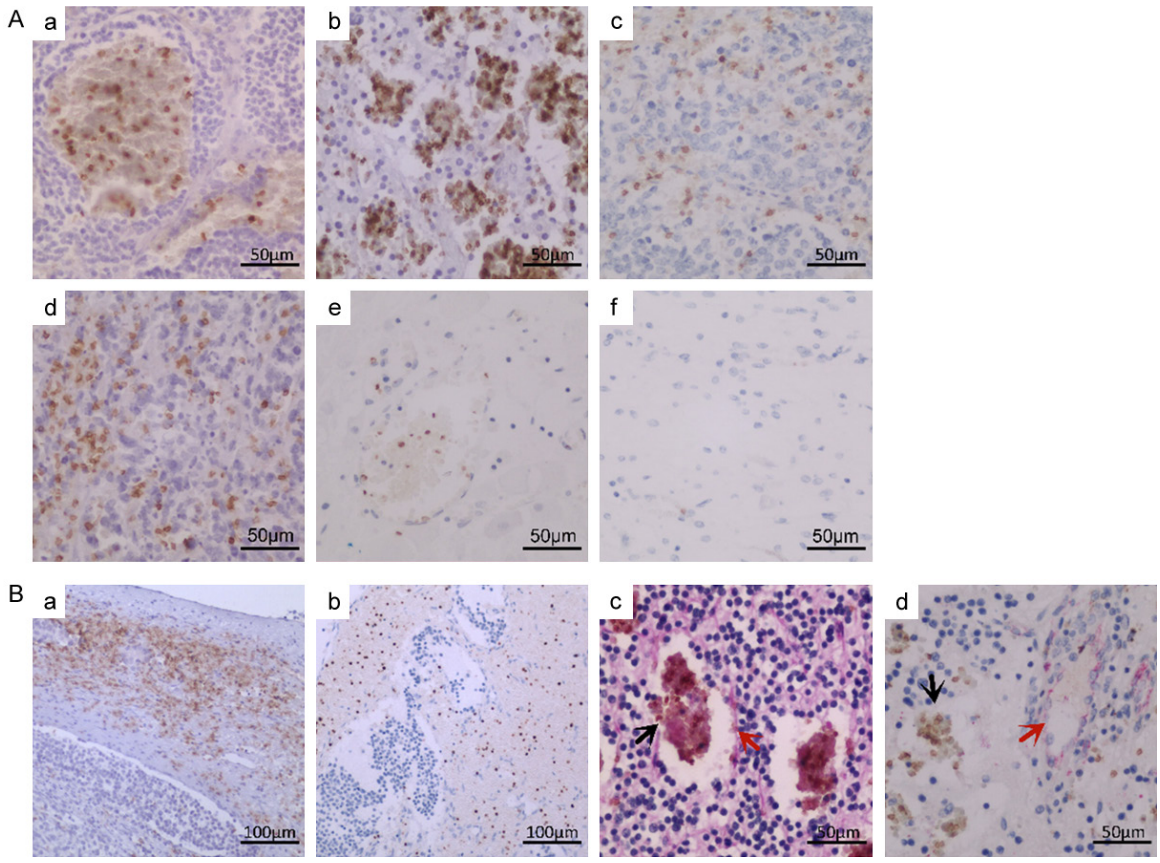

Figure 2. A. Fetal hemoglobin (HB-F) expression in peripheral neuroblastic tumors (pNTs) with different degrees of differentiation: (a) Undifferentiated neuroblastoma (NB) showing moderate expression of HB-F (IHC, ×20). (b) Poorly differentiated NB showing high expression of HB-F (IHC, ×20). (c) Differentiating NB showing moderate expression of HB-F (IHC, ×20). (d) Ganglioneuroblastoma nodular (GNBn) showing moderate expression of HB-F in the nodules (IHC, ×20). (e) Ganglioneuroblastoma intermixed (GNBi) showing low expression of HB-F (IHC, ×20). (f) Ganglioneuroma (GN) showing no expression of HB-F (IHC, ×20). B. HB-F expression at different locations in pNTs: (a) Positive HB-F staining in tumor envelope area (IHC, ×10). (b) Positive HB-F staining around a necrotic area (IHC, ×10). (c) Brown positive HB-F staining (black arrowheads) in the vasculogenic mimicry (VM), with a periodic acid-Schiff (PAS)-positive basement membrane (red arrowheads, HB-F/PAS, ×20). (d) Negative HB-F staining (red arrowheads) in tumor vessels, with brown positive HB-F staining nearby (black arrowheads, HB-F/CD31, ×20).

differentiated histopathological types tended to have higher HB-F expression. According to the group-group comparison, as with VM, the expression of HB-F in poorly differentiated NB was significantly higher than that in the other groups, and HB-F expression in differentiating NB was higher than that in GN; however, there was no significant difference in HB-F expression between differentiating NB and GNBi, or between GNBi and GN (**Table 5**). The HB-F expression was higher in the poor prognosis group than in the good prognosis group ($P< 0.001$, **Table 4**). There was no significant difference in HB-F expression in pNTs according to the MKI ($P=0.658$, **Table 4**).

Correlation between the number of vasculogenic mimicries and fetal hemoglobin expression in peripheral neuroblastic tumors

To further validate the correlation between number of VMs, HB-F expression, and pNT differentiation, we generated bar and scatter plots by ranking the first five groups according to their degree of differentiation. Both VM numbers and HB-F expression showed a decreasing trend with better differentiation (**Figure 3A**, **3B**). Scatter plots showed that the VM number was positively associated with HB-F expression ($r^2=0.847$, **Figure 3C**). Owing to pNT differentiation, HB-F expression was related to age;

Table 2. Relationship between the amount of vasculogenic mimicry and clinical pathological indexes in the peripheral neuroblastic tumors

	n	Number of VMs Me (min, max)	Z/Hc	P
Gender				
Male	50	111.5 (0, 231)	-1.673	0.094
Female	51	54 (0, 220)		
Differentiation type				
Poorly differentiated NB	42	137 (73, 221)	83.279	0.000
Differentiating NB	16	90.5 (14, 135)		
GNBi	24	6.0 (0, 54)		
GN	16	0 (0, 0)		
Prognosis				
Good	83	54 (0, 220)	3.724	0.000
Poor	18	131 (93, 231)		
MKI				
Low	42	121.5 (12, 231)	3.485	0.175
Medium	14	119 (73, 183)		
High	5	151 (140, 167)		

Remarks: VM, vasculogenic mimicry; NB, neuroblastoma; GNBi, ganglioneuroblastoma intermixed; GN, ganglioneuroma; MKI, mitosis-Karyorrhexis index.

Table 3. Group-group comparison of the amount of vasculogenic mimicry in peripheral neuroblastic tumors according to the tissue differentiation type

Group-group	Standard error	Standard test statistics	P
1-2	8.306	3.051	0.014*
1-3	7.234	6.796	0.000**
1-4	8.306	7.796	0.000**
2-3	9.125	2.611	0.054
2-4	9.995	3.942	0.000**
3-4	9.125	1.708	0.526

Remarks: 1 shows poorly differentiated neuroblastoma, 2 shows differentiating neuroblastoma, 3 shows ganglioneuroblastoma intermixed, 4 shows ganglioneuroma, *<0.05, **<0.01.

therefore, we used age as the control variable and performed a partial correlation analysis of the three variables (r=0.891, P<0.001). The results showed that the number of VMs was remained positively correlated with HB-F expression.

Discussion

PNTs are common extracranial malignant solid tumors in children [29]. The pathogenesis of this condition is complex. Owing to its biological heterogeneity, pNTs have diverse clinical manifestations and pathological types, and the prognosis varies [30, 31]. For some pNTs with a good prognosis, the neuroblasts in the tumor body can subside spontaneously during the development process, and the children can be cured by surgical resection of the tumor, whereas for some pNTs with a poor prognosis, metastasis and recurrence can still occur despite tumor body resection, radiotherapy, chemotherapy, and combined treatments [30]. Exploring the mechanism of drug resistance in the treatment of high-risk NB has become an important and challenging research topic in recent years. We studied 101 tissue samples with pNTs and demonstrated the presence of VM and its relationship to the degree of differentiation. The number of VMs in poorly differentiated tumors was significantly higher than that in well-differentiated tumors. Statistical analysis revealed that the number of VMs in the poor prognosis group was significantly higher than that in the good prognosis group, indicating that the presence of VMs is also a risk factor for poor prognosis in pNTs. The VM was mostly concentrated under the capsule, and at the edge of necrotic areas, in areas with more neuroblasts. These areas are the most prone to hypoxia. The hypoxic microenvironment stimulates tumor cells to form VM through various mechanisms, thereby providing rapid blood support for tumor cells. In some other malignant tumors, the mechanism of VM had been confirmed to involve processes such as cytoskeleton reorganization caused by matrix metalloproteinases, HIF-1α promote epithelial-mesenchymal transition, high expression of lncRNA, and immune proteins related to tumor recruitment [32-35], but further research is needed to confirm the mechanism of VM formation in pNTs. Villasante et al. [28] established an in vitro vascularized tissue engineering model to confirm that there are two types of VM: (1) a vascular-like structure formed by tumor cells surrounding erythrocytes with $CD31^-/PAS^+$ lumen wall cells; and (2) a blood vessel formed by tumor-derived endothelial cells with $CD31^+$ lumen wall cells. Isotretinoin

Table 4. Relationship between the expression of fetal hemoglobin and clinical pathological indexes in peripheral neuroblastic tumors

	n	HB-F (%) Me (min, max)	Z/Hc	P
Gender				
Male	50	14.5 (0, 47)	-1.863	0.062
Female	51	2.2 (0, 55)		
Differentiation type				
Poorly differentiated NB	42	25.5 (5.0, 55.0)	84.195	0.000
Differentiating NB	16	8.5 (1.0, 14.0)		
GNBi	24	1.0 (0, 5.0)		
GN	16	0.0 (0, 1.0)		
Prognosis				
Good	83	4.0 (0, 55)	3.674	0.000
Poor	18	20 (5, 47)		
MKI				
Low	42	19.5 (1, 55)	0.836	0.658
Medium	14	22 (5, 43)		
High	5	20 (11.3, 42)		

Remarks: HB-F, fetal hemoglobin; NB, neuroblastoma; GNBi, ganglioneuroblastoma intermixed; GN, ganglioneuroma; MKI, mitosis-Karyorrhexis index.

Table 5. Group-group comparison of the expression of fetal hemoglobin in peripheral neuroblastic tumors according to the tissue differentiation type

Group-group	Standard error	Standard test statistics	P
1-2	8.310	3.469	0.003**
1-3	7.238	7.134	0.000**
1-4	8.310	7.516	0.000**
2-3	9.129	2.498	0.075
2-4	10.000	3.362	0.005**
3-4	9.129	1.186	1.000

Remarks: 1 shows poorly differentiated neuroblastoma, 2 shows differentiating neuroblastoma, 3 shows ganglioneuroblastoma intermixed, 4 shows ganglioneuroma, **<0.01.

was ineffective for treating both VM types, suggesting that VM contributes to neuroblastoma drug resistance. The second type of VM has been confirmed in several studies [36]. We confirmed the existence of the first type of VM in pNTs by CD31/PAS double staining. To our knowledge, this is the first study to confirm the relationship between the number of VMs and the histopathological type in natural pNTs. It appears that for pNTs, tumors with VMs are more prone to hematogenous metastasis and have a poor prognosis, which may be related to treatment resistance.

HB-F is the main protein in fetal red blood cells, accounting for approximately 95% of total hemoglobin in the middle and late trimesters of pregnancy, and decreases to approximately 70% directly after birth. HB-F then gradually decreases to less than 10% of total hemoglobin by the age of 4 months, and continues to decrease until it falls to the adult level (<2%) and then stabilizes [37, 38]. An elevated level of HB-F in the blood is a sign of hematologic disease or a malignant tumor [39]. Immunohistochemical staining has confirmed that extravascular HB-F-positive aggregation also occurs in some malignant solid tumors and that the production of HB-F does not originate from systemic blood circulation [27]. Recently, Zhang et al. [40, 41] reported that cell lines of some tumors, such as breast cancer and colorectal cancer, can form polyploid giant cancer cells (PGCCs) after in vitro induction. These PGCCs have the characteristics of stem cell-like cells, can produce erythroid cells in vitro and in vivo, and activate the expression of HB-F or embryonic hemoglobin [41, 42]. HB-F is composed of globin ($2\alpha2\gamma$ tetramer) and heme, with a γ chain instead of a β chain as in adult hemoglobin. The chain structure of HB-F has a better affinity for oxygen [43]. The activated expression of erythroid differentiation-related proteins can increase the ability of cells to obtain oxygen in a hypoxic microenvironment, thereby promoting tumor growth. PGCCs, their daughter cells, and surrounding tumor cells can also form VM structures around the erythroid cells that they produce, which can connect endothelium-dependent vessels to obtain sufficient blood and oxygen to promote tumor growth, invasion, and metastasis. This shows the importance of HB-F in tumor growth. This study found that tumor cells in pNTs had different levels of HB-F expression, and that the expression of HB-F increased significantly as the level of tumor differentiation decreased. The expression of HB-F was related

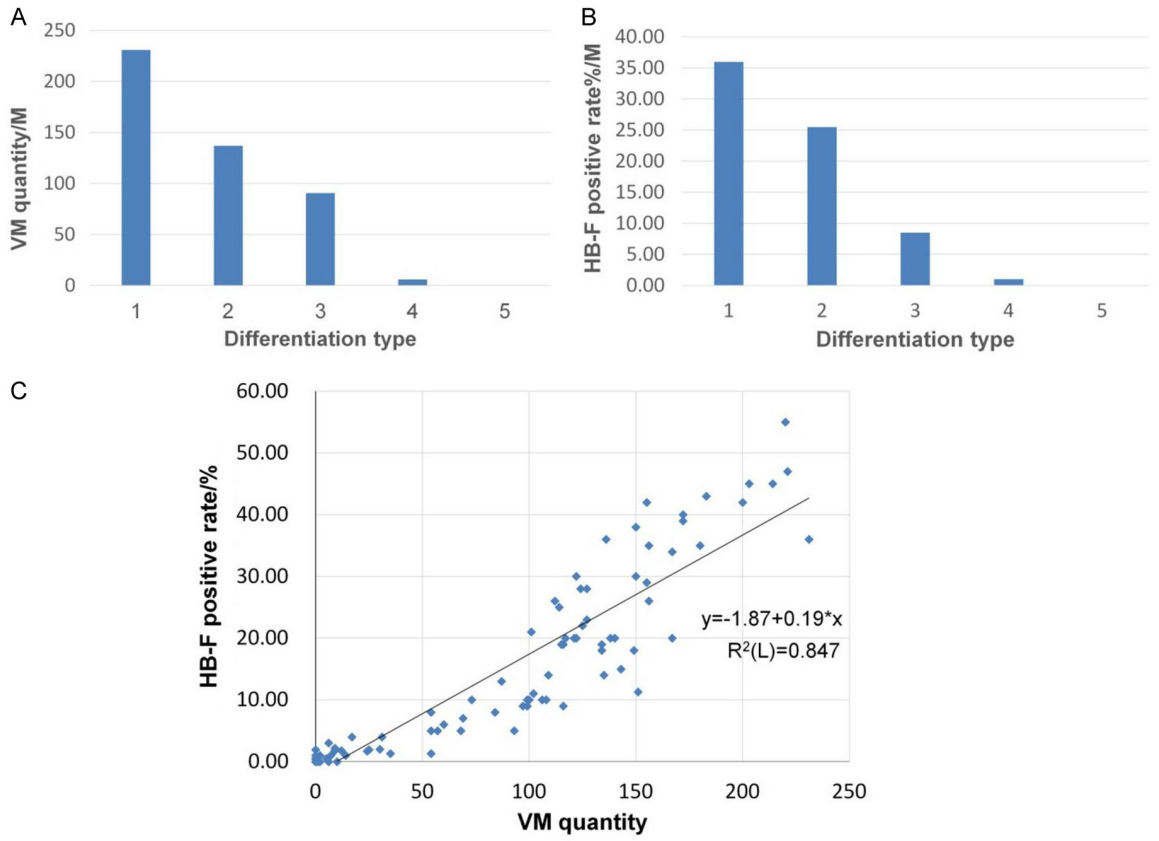

Figure 3. A. The relationship between tumor differentiation and vasculogenic mimicry (VM) in peripheral neuroblastic tumors (pNTs) (1 shows undifferentiated neuroblastoma, 2 shows poorly differentiated neuroblastoma, 3 shows differentiating neuroblastoma, 4 shows ganglioneuroblastoma intermixed, 5 shows ganglioneuroma). B. The relationship between tumor differentiation and fetal hemoglobin (HB-F) expression levels in pNTs (1 shows undifferentiated neuroblastoma, 2 shows poorly differentiated neuroblastoma, 3 shows differentiating neuroblastoma, 4 shows ganglioneuroblastoma intermixed, 5 shows ganglioneuroma). C. The correlation between VM and HB-F expression in 101 children with pNTs.

to prognosis, and a high level of HB-F expression was also a risk factor for poor prognosis. There was a strong positive correlation between HB-F expression and the number of VMs. The HB-F-positive component was distributed primarily in the parts of the tumor where the hypoxia was more likely to be a problem (such as the front of tumor invasion and around the necrotic area or in the VM), which was similar to the distribution area of VMs, suggesting that there are similarities in the production mechanism of HB-F and VM. Studies have confirmed that in embryonic tumors, some erythrocytes expressing HB-F are in mitosis, which may be related to the primitive embryo-like characteristics of the tumor. These tumor cells have stem cell-like characteristics that can promote the development of erythrocyte precursors or induce HB-F biosynthesis through an unknown mechanism. Therefore, we hypothesize that some neuroblasts in the pNTs may have stem cell-like characteristics, and that under hypoxic conditions, these cells produce erythrocytes and express HB-F. Neuroblasts can form VM around these erythrocytes to provide blood and oxygen support to tumors to promote tumor growth and metastasis. The specific mechanism of VM and tumor cell expression of HB-F in pNTs requires further experimental research.

Conclusion

In conclusion, to our knowledge, this is the first study to confirm a relationship between VM, HB-F expression, and the pNT pathological type. The increase in the number of VMs and expression of HB-F are related to the differentiation type and prognosis of pNTs. Further

studies of the mechanisms of pNTs may lead to the discovery of new methods to improve tumor prognosis and reduce drug resistance.

Acknowledgements

This work was supported in part by grants from the National Science Foundation of China (#82173283 and #82103088), and Foundation of committee on science and technology of Tianjin (#20JCYBJC01230). The funders had no roles in the design of the study, data collection, analysis and interpretation, or decision to write and publish the work. We acknowledge Editage service for the manuscript language edit.

Disclosure of conflict of interest

None.

Abbreviations

VM, vasculogenic mimicry; HB-F, fetal hemoglobin; pNTs, peripheral neuroblastic tumors; NB, neuroblastoma; GNBi, ganglioneuroblastoma intermixed; GN, ganglioneuroma; INPC, International Neuroblastoma Pathology Committee; GNBn, ganglioneuroblastoma nodular; MKI, mitosis-Karyorrhexis index; FH, favorable histology; UH, unfavorable histology; H&E, hematoxylin and eosin; PAS, periodic acid-Schiff; DAB, diaminobenzidine; PGCCs, polyploid giant cancer cells.

Address correspondence to: Dr. Shiwu Zhang, Department of Pathology, Tianjin Union Medical Center, Tianjin 300121, China. Tel: +86-15620876109; Fax: +86-022-87721989; E-mail: zhangshiwu666@aliyun.com

References

[1] Liu Z and Thiele CJ. Unraveling the enigmatic origin of neuroblastoma. Cancer Cell 2020; 38: 618-620.

[2] Calero R, Morchon E, Johnsen JI and Serrano R. Sunitinib suppress neuroblastoma growth through degradation of MYCN and inhibition of angiogenesis. PLoS One 2014; 9: e95628.

[3] Salemi F, Alam W, Hassani MS, Hashemi SZ, Jafari AA, Mirmoeeni SMS, Arbab M, Mortazavizadeh SMR and Khan H. Neuroblastoma: essential genetic pathways and current therapeutic options. Eur J Pharmacol 2022; 926: 175030.

[4] Park JR, Eggert A and Caron H. Neuroblastoma: biology, prognosis, and treatment. Pediatr Clin North Am 2008; 55: 97-120, x.

[5] Shimada H, Ambros IM, Dehner LP, Hata J, Joshi VV and Roald B. Terminology and morphologic criteria of neuroblastic tumors: recommendations by the International Neuroblastoma Pathology Committee. Cancer 1999; 86: 349-363.

[6] Kong J, Sertel O, Shimada H, Boyer KL, Saltz JH and Gurcan MN. Computer-aided evaluation of neuroblastoma on whole-slide histology images: classifying grade of neuroblastic differentiation. Pattern Recognit 2009; 42: 1080-1092.

[7] Peuchmaur M, d'Amore ES, Joshi VV, Hata J, Roald B, Dehner LP, Gerbing RB, Stram DO, Lukens JN, Matthay KK and Shimada H. Revision of the international neuroblastoma pathology classification: confirmation of favorable and unfavorable prognostic subsets in ganglioneuroblastoma, nodular. Cancer 2003; 98: 2274-2281.

[8] Beiske K, Burchill SA, Cheung IY, Hiyama E, Seeger RC, Cohn SL, Pearson AD and Matthay KK; International neuroblastoma Risk Group Task Force. Consensus criteria for sensitive detection of minimal neuroblastoma cells in bone marrow, blood and stem cell preparations by immunocytology and QRT-PCR: recommendations by the International Neuroblastoma Risk Group Task Force. Br J Cancer 2009; 100: 1627-1637.

[9] Yang L, Li Y, Wei Z and Chang X. Coexpression network analysis identifies transcriptional modules associated with genomic alterations in neuroblastoma. Biochim Biophys Acta Mol Basis Dis 2018; 1864: 2341-2348.

[10] Nakazawa A. Biological categories of neuroblastoma based on the international neuroblastoma pathology classification for treatment stratification. Pathol Int 2021; 71: 232-244.

[11] Goto S, Umehara S, Gerbing RB, Stram DO, Brodeur GM, Seeger RC, Lukens JN, Matthay KK and Shimada H. Histopathology (international neuroblastoma pathology classification) and MYCN status in patients with peripheral neuroblastic tumors: a report from the Children's Cancer Group. Cancer 2001; 92: 2699-2708.

[12] Nakazawa A, Haga C, Ohira M, Okita H, Kamijo T and Nakagawara A. Correlation between the international neuroblastoma pathology classification and genomic signature in neuroblastoma. Cancer Sci 2015; 106: 766-771.

[13] Ponzoni M, Bachetti T, Corrias MV, Brignole C, Pastorino F, Calarco E, Bensa V, Giusto E, Ceccherini I and Perri P. Recent advances in the developmental origin of neuroblastoma: an overview. J Exp Clin Cancer Res 2022; 41: 92.

[14] Whittle SB, Smith V, Doherty E, Zhao S, McCarty S and Zage PE. Overview and recent advances in the treatment of neuroblastoma.

Expert Rev Anticancer Ther 2017; 17: 369-386.
[15] Sun B, Zhang D, Zhang S, Zhang W, Guo H and Zhao X. Hypoxia influences vasculogenic mimicry channel formation and tumor invasion-related protein expression in melanoma. Cancer Lett 2007; 249: 188-197.
[16] Ayala-Domínguez L, Olmedo-Nieva L, Muñoz-Bello JO, Contreras-Paredes A, Manzo-Merino J, Martínez-Ramírez I and Lizano M. Mechanisms of vasculogenic mimicry in ovarian cancer. Front Oncol 2019; 9: 998.
[17] Li H, Wang D, Yi B, Cai H, Wang Y, Lou X, Xi Z and Li Z. SUMOylation of IGF2BP2 promotes vasculogenic mimicry of glioma via regulating OIP5-AS1/miR-495-3p axis. Int J Biol Sci 2021; 17: 2912-2930.
[18] Andonegui-Elguera MA, Alfaro-Mora Y, Cáceres-Gutiérrez R, Caro-Sánchez CHS, Herrera LA and Díaz-Chávez J. An overview of vasculogenic mimicry in breast cancer. Front Oncol 2020; 10: 220.
[19] Zheng N, Zhang S, Wu W, Zhang N and Wang J. Regulatory mechanisms and therapeutic targeting of vasculogenic mimicry in hepatocellular carcinoma. Pharmacol Res 2021; 166: 105507.
[20] You X, Wu J, Wang Y, Liu Q, Cheng Z, Zhao X, Liu G, Huang C, Dai J, Zhou Y, Chen D and Chong Y. Galectin-1 promotes vasculogenic mimicry in gastric adenocarcinoma via the Hedgehog/GLI signaling pathway. Aging (Albany NY) 2020; 12: 21837-21853.
[21] Wu M, Sun X, Wang T, Zhang M and Li P. TRPS1 knockdown inhibits angiogenic vascular mimicry in human triple negative breast cancer cells. Clin Transl Oncol 2022; 24: 145-153.
[22] Xu MR, Wei PF, Suo MZ, Hu Y, Ding W, Su L, Zhu YD, Song WJ, Tang GH, Zhang M and Li P. Brucine suppresses vasculogenic mimicry in human triple-negative breast cancer cell line MDA-MB-231. Biomed Res Int 2019; 2019: 6543230.
[23] Mahdi A, Darvishi B, Majidzadeh AK, Salehi M and Farahmand L. Challenges facing antiangiogenesis therapy: the significant role of hypoxia-inducible factor and MET in development of resistance to anti-vascular endothelial growth factor-targeted therapies. J Cell Physiol 2019; 234: 5655-5663.
[24] Soda Y, Myskiw C, Rommel A and Verma IM. Mechanisms of neovascularization and resistance to anti-angiogenic therapies in glioblastoma multiforme. J Mol Med (Berl) 2013; 91: 439-448.
[25] Serova M, Tijeras-Raballand A, Dos Santos C, Martinet M, Neuzillet C, Lopez A, Mitchell DC, Bryan BA, Gapihan G, Janin A, Bousquet G, Riveiro ME, Bieche I, Faivre S, Raymond E and de Gramont A. Everolimus affects vasculogenic mimicry in renal carcinoma resistant to sunitinib. Oncotarget 2016; 7: 38467-38486.
[26] Pritišanac E, Urlesberger B, Schwaberger B and Pichler G. Fetal hemoglobin and tissue oxygenation measured with near-infrared spectroscopy-a systematic qualitative review. Front Pediatr 2021; 9: 710465.
[27] Wolk M, Martin JE and Nowicki M. Foetal haemoglobin-blood cells (F-cells) as a feature of embryonic tumours (blastomas). Br J Cancer 2007; 97: 412-419.
[28] Villasante A, Sakaguchi K, Kim J, Cheung NK, Nakayama M, Parsa H, Okano T, Shimizu T and Vunjak-Novakovic G. Vascularized tissue-engineered model for studying drug resistance in neuroblastoma. Theranostics 2017; 7: 4099-4117.
[29] Yang T, Li J, Zhuo Z, Zeng H, Tan T, Miao L, Zheng M, Yang J, Pan J, Hu C, Zou Y, He J and Xia H. TTF1 suppresses neuroblastoma growth and induces neuroblastoma differentiation by targeting TrkA and the miR-204/TrkB axis. iScience 2022; 25: 104655.
[30] Gonçalves-Alves E, Garcia M, Rodríguez-Hernández CJ, Gómez-González S, Ecker RC, Suñol M, Muñoz-Aznar O, Carcaboso AM, Mora J, Lavarino C and Mateo-Lozano S. AC-265347 inhibits neuroblastoma tumor growth by induction of differentiation without causing hypocalcemia. Int J Mol Sci 2022; 23: 4323.
[31] Altungoz O, Aygun N, Tumer S, Ozer E, Olgun N and Sakizli M. Correlation of modified Shimada classification with MYCN and 1p36 status detected by fluorescence in situ hybridization in neuroblastoma. Cancer Genet Cytogenet 2007; 172: 113-119.
[32] Li Y, Sun B, Zhao X, Wang X, Zhang D, Gu Q and Liu T. MMP-2 and MMP-13 affect vasculogenic mimicry formation in large cell lung cancer. J Cell Mol Med 2017; 21: 3741-3751.
[33] Li W, Zong S, Shi Q, Li H, Xu J and Hou F. Hypoxia-induced vasculogenic mimicry formation in human colorectal cancer cells: involvement of HIF-1a, Claudin-4, and E-cadherin and Vimentin. Sci Rep 2016; 6: 37534.
[34] Li Y, Wu Z, Yuan J, Sun L, Lin L, Huang N, Bin J, Liao Y and Liao W. Long non-coding RNA MALAT1 promotes gastric cancer tumorigenicity and metastasis by regulating vasculogenic mimicry and angiogenesis. Cancer Lett 2017; 395: 31-44.
[35] Liu X, Lv Z, Zhou S, Kan S, Liu X, Jing P and Xu W. MTDH in macrophages promotes the vasculogenic mimicry via VEGFA-165/Flt-1 signaling pathway in head and neck squamous cell carcinoma. Int Immunopharmacol 2021; 96: 107776.

[36] Pezzolo A, Parodi F, Corrias MV, Cinti R, Gambini C and Pistoia V. Tumor origin of endothelial cells in human neuroblastoma. J Clin Oncol 2007; 25: 376-383.
[37] Dana M and Fibach E. Fetal hemoglobin in the maternal circulation - contribution of fetal red blood cells. Hemoglobin 2018; 42: 138-140.
[38] Bard H. The postnatal decline of hemoglobin F synthesis in normal full-term infants. J Clin Invest 1975; 55: 395-398.
[39] Wolk M, Martin JE and Constantin R. Blood cells with fetal haemoglobin (F-cells) detected by immunohistochemistry as indicators of solid tumours. J Clin Pathol 2004; 57: 740-745.
[40] Zhang S, Mercado-Uribe I and Liu J. Generation of erythroid cells from fibroblasts and cancer cells in vitro and in vivo. Cancer Lett 2013; 333: 205-212.
[41] Zhang D, Yang X, Yang Z, Fei F, Li S, Qu J, Zhang M, Li Y, Zhang X and Zhang S. Daughter cells and erythroid cells budding from PGCCs and their clinicopathological significances in colorectal cancer. J Cancer 2017; 8: 469-478.
[42] Li Z, Zheng M, Zhang H, Yang X, Fan L, Fu F, Fu J, Niu R, Yan M and Zhang S. Arsenic trioxide promotes tumor progression by inducing the formation of PGCCs and embryonic hemoglobin in colon cancer cells. Front Oncol 2021; 11: 720814.
[43] Manning JM, Manning LR, Dumoulin A, Padovan JC and Chait B. Embryonic and fetal human hemoglobins: structures, oxygen binding, and physiological roles. Subcell Biochem 2020; 94: 275-296.